Kovove Mater. 58 2020 121–128
DOI: 10.4149/km_2020_2_121

Microstructure evolution and properties of reheated coarse grain heat-affected zone of 900 MPa grade HSLA steel

H. Qin[1]*, Z. Qiao[1], Q. Wu[1], J. Lian[1], L. Wang[1], Y. Cui[2]

[1] *School of Mechanical Engineering, Liaoning Shihua University, Fushun 113001, P. R. China*
[2] *Fushun Petrochemical Company Petroleum Third Factory, Liaoning Fushun 113001, P. R. China*

Received 8 November 2019, received in revised form 22 January 2020, accepted 24 January 2020

Abstract

The welding thermal simulation technology was used to simulate secondary thermal cycle of coarse grain heat-affected zone (CGHAZ) of BWELDY960Q steel, and the change of microstructure and toughness in CGHAZ after reheating was studied in detail. The results show that when the peak temperature of the secondary thermal cycle is 1200 and 1000 °C, the microstructure of reheated coarse grain heat-affected zone (RCGHAZ) is martensite; when the peak temperature is 800 °C, the microstructure of RCGHAZ constitutes of martensite, granular bainite and M-A constituent. The toughness of CGHAZ is improved undergoing secondary thermal cycle, but it is still lower than that of base metal. Compared with the mechanical properties of CGHAZ, the hardness values of inter-critical and sub-critical RCGHAZ are decreased, while the toughness of super-critical and sub-critical RCGHAZ is increased. Impact fracture exhibits evident plastic deformation, the edge of fracture has tearing edges and corners, and microscopic morphology presents the characteristics of dimp fracture.

K e y w o r d s: HSLA steel, reheated coarse grain heat-affected zone, microstructure, properties

1. Introduction

BWELDY960Q steel is a low carbon and low alloy high strength steel with good toughness and excellent welding performance, which was usually applied in the engineering fields of bridges, construction, and hydropower. Due to high strength of BWELDY960Q steel, it can reduce the weight of the structural parts and achieve the goal of saving steel, so it has very significant economic benefits. Welding is a key technical issue for the application of low alloy high strength (HSLA) steel. Under various welding conditions, some problems, such as cold cracking in welded joints and the toughness of heat-affected zone (HAZ) is asked to improve, and crack is prevented [1–5]. Because HAZ undergoes welding thermal cycling, its properties are different from those of base metal, and directly affect whether the welded joints can be safely applied [6–10].

In the engineering, multi-layer and multi-pass welding is often used to weld low alloy high strength steel to obtain welded joints, and multi-layer welding is constituted by many single-layer welding thermal cycles; therefore the secondary thermal cycle during the welding process has a certain impact on the microstructure and properties of HAZ.

By simulating a thermal cycle test, it is known that the CGHAZ of BWELDY960Q steel has relatively low impact toughness and becomes the most severely embrittled zone in HAZ. The welding thermal simulation technology is used to further study the change of microstructure and properties of CGHAZ after the secondary thermal cycle, which provided a basis for the development of reasonable welding process and engineering application.

2. Experimental procedures

2.1. Materials

BWELDY960Q steel was used for experimental material, which processed with the heating tempe-

*Corresponding author: e-mail address: huaq2008@163.com

Table 1. Chemical composition of BWELDY960Q steel (mass%)

Steel	C	Si	Mn	S	P	Cr	Ni	Mo	Nb	V	Ti	B
BWELDY960Q	0.18	0.50	1.60	0.01	0.02	0.08	1.00	0.60	0.05	0.05	0.03	0.005

Table 2. Mechanical properties of experimental steel

Steel	Yield strength (MPa)	Tensile strength (MPa)	Elongation	Impact toughness (J) –20 °C
BWELDY960Q	960	980	12 %	102

Table 3. Welding thermal simulation parameters

	Temperature T_{p1} (°C)	Temperature T_{p2} (°C)	Heating rate ω_H (°C s^{-1})	Holding time t_H (s)	Heat input q (kJ cm^{-1})
URCGHAZ	1320	1200	103	2	10
SCRCGHAZ	1320	1000	103	2	
IRCGHAZ	1320	800	103	2	
SRCGHAZ	1320	600	103	2	

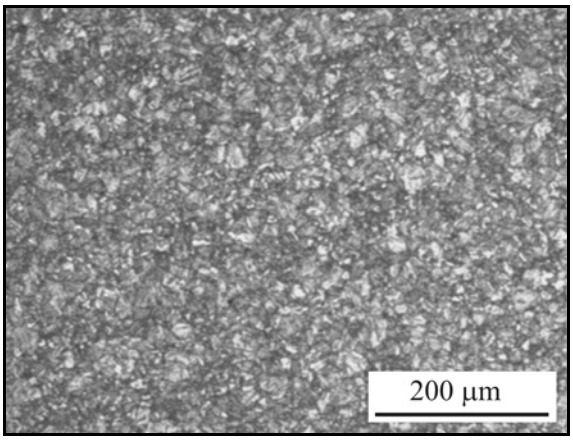

Fig. 1. The microstructure of BWELDY960Q steel.

rature at 900 °C for 2 h and tempering to 650 °C for 1 h. The microstructure of experimental steel was tempered sorbate, as shown in Fig. 1. The chemical composition of BWELDY960Q steel is shown in Table 1. The experimental steel has the yield strength of 960 MPa and tensile strength of 980 MPa, and its critical phase transition temperature A_{c1} is 725 °C and A_{c3} is 876 °C.

2.2. Methods

The test was carried out by using the Gleeble 1500 thermo-mechanical simulator to simulate the thermal cycling test. The peak temperature T_{p1} of a thermal cycle was 1320 °C, and the peak temperature T_{p2} of the secondary thermal cycle is 1200, 1000, 800, and 600 °C, respectively, for unaltered reheated coarse grain heat-affected zone (URCGHAZ), super-critical reheated coarse grain heat-affected zone (SCRCGHAZ), inter-critical reheated coarse grain heat-affected zone (IRCGHAZ), and sub-critical reheated coarse grain heat-affected zone (SRCGHAZ). Table 3 lists the thermal simulation test parameters, and Fig. 2 presents the thermal cycle curves at different temperatures. The actual welded joint was obtained with 80%Ar + 20%CO_2 as a protective gas for multi-layer and multi-pass welding. The plate thickness was 10 mm, and the heat input was 10 kJ cm^{-1}.

The sample subjected to the secondary thermal cycle was processed into a standard sample of 55 mm × 10 mm × 10 mm with a V-notch opened at the thermocouple spot welding position, and JB-30B type impact test machine was used to impact test at –20 °C in accordance with GB/T229-2007. All the simulated samples were ground, polished, and etched with 4 % (volume fraction) nitric acid solution to observe microstructure by optical microscope (OM) and scanning electron microscope (SEM). The simulated sample with peak temperature of 800 °C was cut into 1 mm thin slices by wire cutting, and transmission electron microscopy (TEM) sample was prepared by mechanical thinning and electrolytic double spraying with 10 % (volume fraction) perchloric acid alcohol solution as the electrolytic double spray, voltage 18 V and temperature –20 °C.

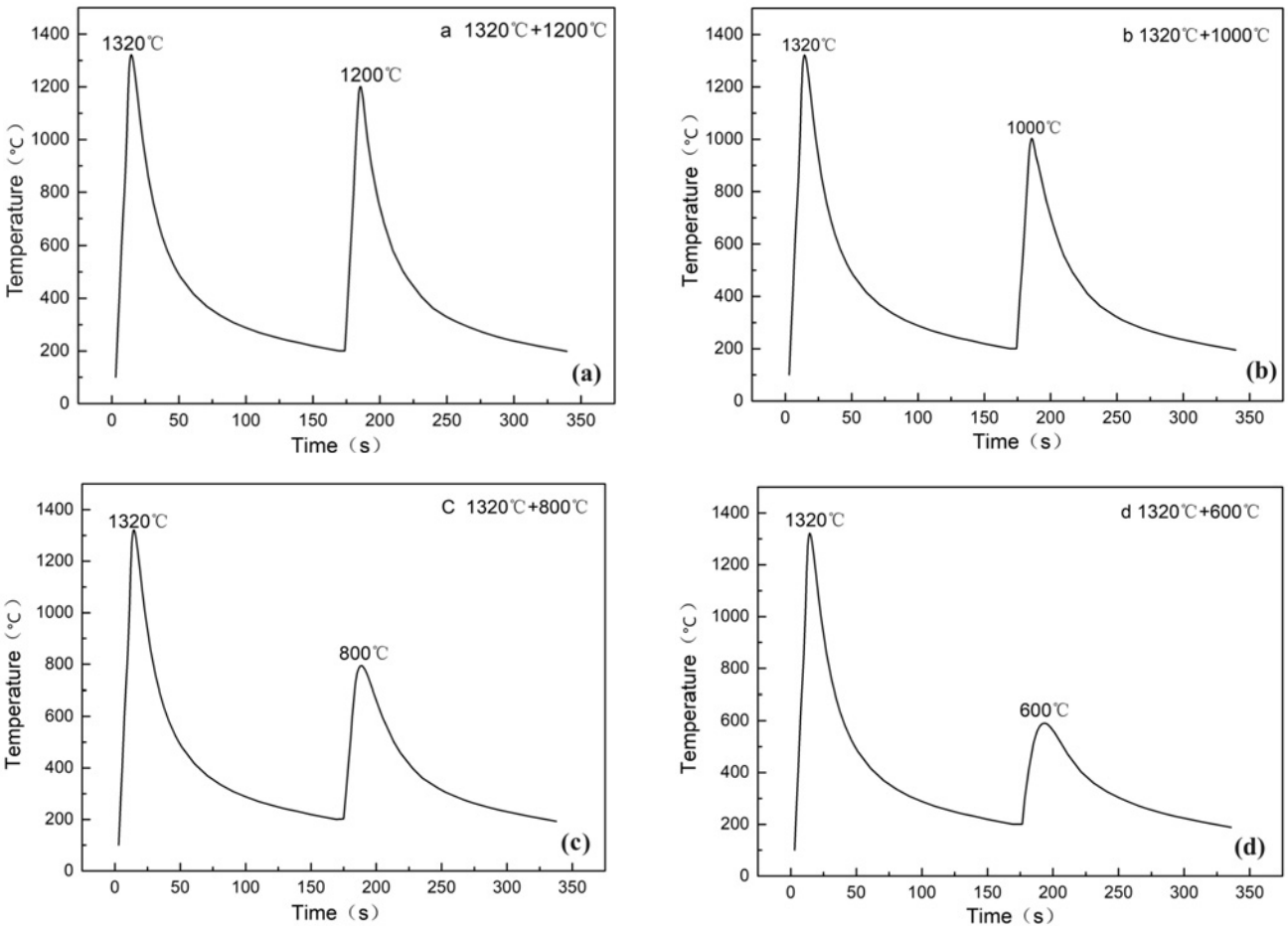

Fig. 2. Thermal cycle curve of reheating coarse grain heat-affected zone: URCGHAZ (a), SRCGHAZ (b), IRCGHAZ (c), and SCGHAZ (d).

3. Results and discussion

3.1. Microstructure analysis

Figure 3 presents the microstructure of CGHAZ of BWELDY960Q steel. As shown in Fig. 3, the microstructure has the characteristic of the coarse--grained lath martensite (ML). The temperature of a thermal cycle is 1320 ℃, at this time, the heating temperature is much higher than A_{c3}, and the coarse-grained austenite is cooled to obtain coarse lath martensite.

Figure 4 presents the microstructure of reheated coarse grain heat-affected zone (RCGHAZ) at different temperature. When the peak temperature T_{p2} is 1200 ℃, due to the high heating temperature, the prior austenite grain grows significantly; coarse-grain martensite is obtained after cooling. Moreover, the microstructure is not significantly improved; thus, it consists of lath martensite (Fig. 4a). When the peak temperature T_{p2} is 1000 ℃ that is between A_{c3} and 1100 ℃, the coarse grain martensite undergoes heat again, and the prior austenite grains are remarkably refined; therefore fine-grain lath martensite is obtained (Fig. 4b). When the peak temperature T_{p2} is 800 ℃ that is between A_{c1} and A_{c3} because the sample is heated quickly and the holding time is very short under high temperature, only part of the phase trans-

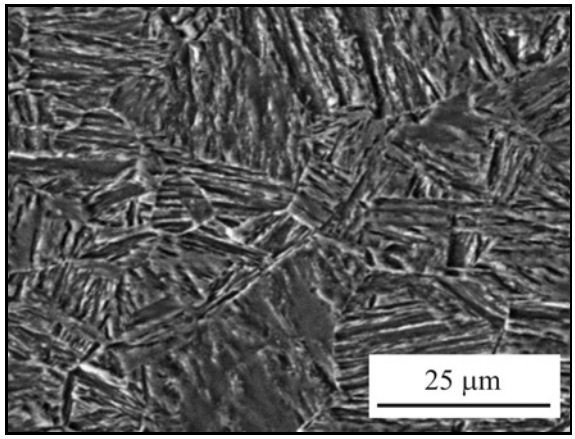

Fig. 3. The microstructure of the coarse grain heat-affected zone.

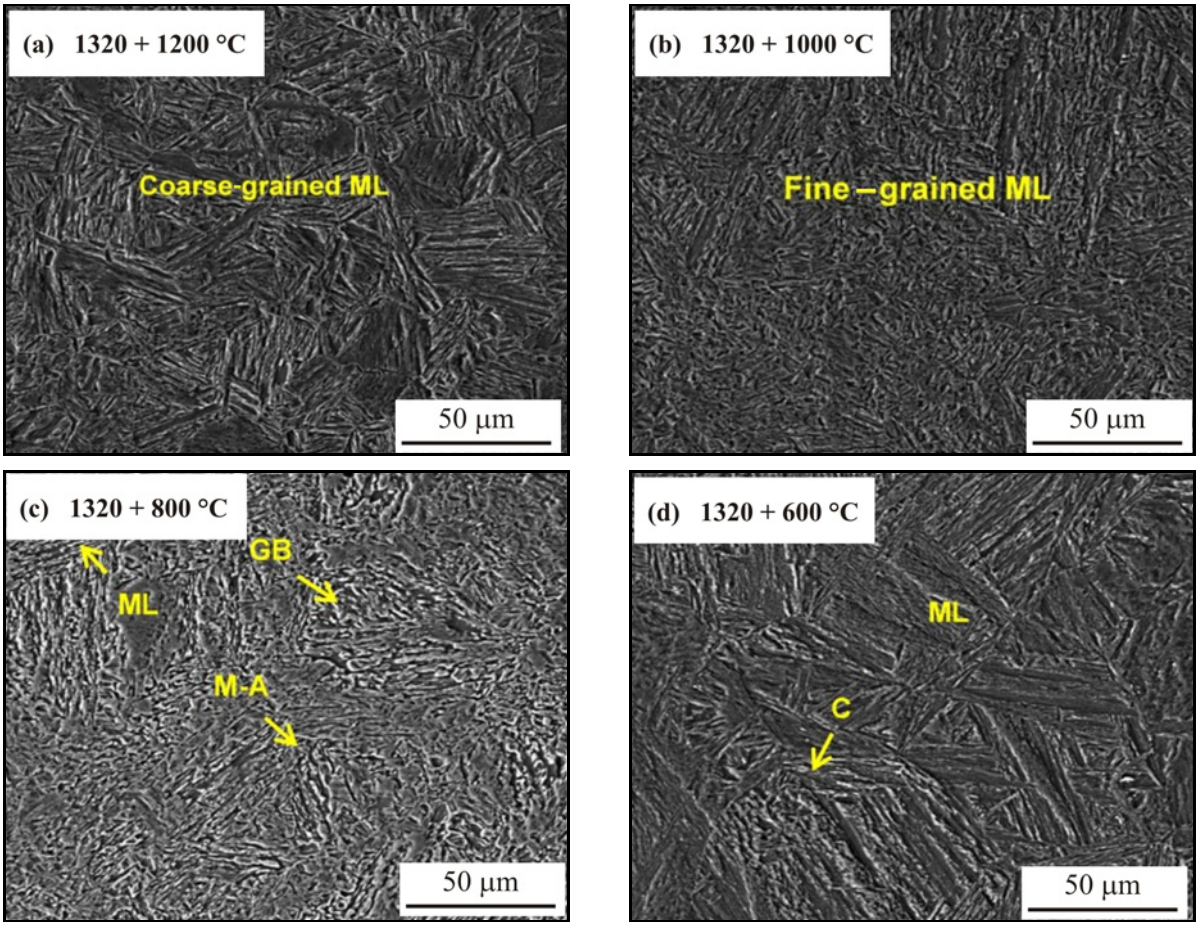

Fig. 4. Microstructure of RCGHAZ at different temperatures: 1320 + 1200 ℃ (a), 1320 + 1000℃ (b), 1320 + 800℃ (c), and 1320 + 600℃ (d).

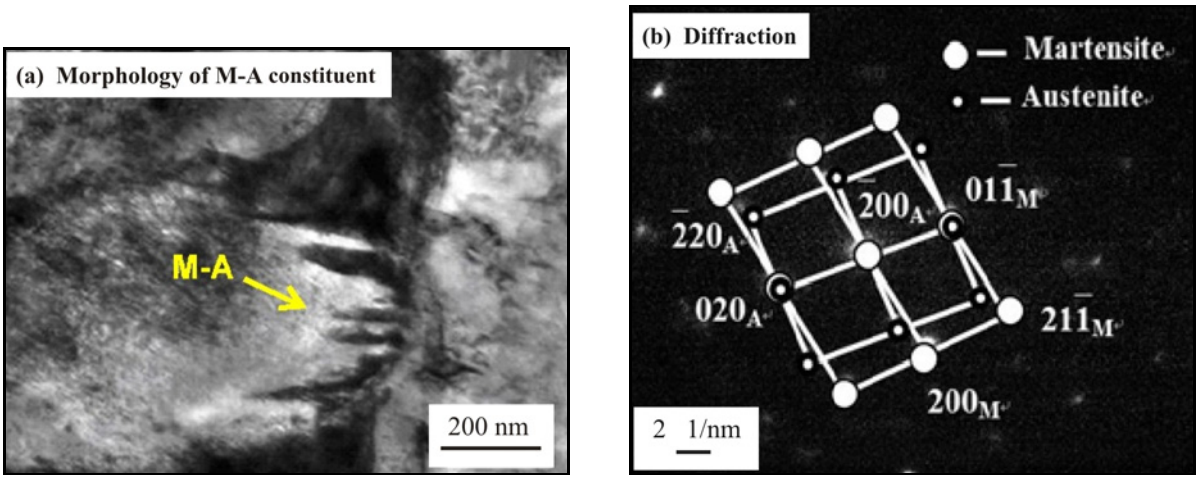

Fig. 5. TEM observation of IRCGHAZ: TEM morphology of M-A constituent (a) and electron diffraction (b).

forms into granular bainite (GB) during the subsequent cooling process, another part of the phase has not changed; therefore a mixed microstructure of martensite and granular bainite occurs. The island phase appears in the mixed microstructure; the discontinuous strips composed of M-A constituent are arranged in parallel on the ferrite matrix (Fig. 4c). When the experimental steel CGHAZ is in the mid-temperature upper bainite transformation zone, the cooling rate is small, and carbon is diffused from the α/γ-phase boundary to γ, the island-shaped M-A constituent surrounded by ferrite is enriched with a large

number of carbon atoms, resulting in higher carbon content of M-A constituent [11–13]. When the peak temperature T_{p2} is 600 ℃ lower than A_{c1} and the sample is subjected to high-temperature tempering, the microstructure is still dominated by lath martensite, and the lath structure is clearly visible (Fig. 4d). When the alloy steel is tempered at a higher temperature, the carbon concentration of the phase is maintained and only a small part of the carbide is precipitated [14–16].

M-A constituent is further observed in the microstructure of IRCGHAZ by using TEM (Fig. 5). The M-A constituent is formed at a moderate cooling rate, and its formation conditions are similar to those of upper bainite (Bu). After the non-equilibrium microstructure of CGHAZ is heated again to the two--phase zone and the amount of austenite increases. During the cooling process, to ensure the stability of austenite, the carbon atoms constantly diffuse into untransformed austenite, leading to a carbon-rich zone formed, and this concentration does not reach the extent of carbide precipitation. The part of the carbon-rich austenite transforms into martensite, the other part is retained austenite, and the M-A constituent is formed [17, 18]. M-A constituent becomes a potential crack source, which causes stress concentration, and an embrittlement appears [19, 20]. From Fig. 5a, we can see that M-A constituent appears at the grain boundary. As shown in Fig. 5b, there are two sets of spots of martensite and austenite in the electron diffraction image, the large white dots are marked as martensite, and the black dots are marked as austenite. When the secondary thermal cycle peak temperature is between A_{c1}–A_{c3}, the M-A constituent appears in IRCGHAZ at the appropriate cooling rate.

3.2. Impact toughness and microhardness

The impact toughness and microhardness of the base metal are 102 J and 383 HV, respectively, and the impact toughness and microhardness of CGHAZ are 18 J and 410 HV, respectively. Figure 6 presents the impact toughness and microhardness of RCGHAZ at different temperature. After CGHAZ undergoes different peak temperature thermal cycles in the secondary thermal cycle, the toughness and microhardness of the CGHAZ have varying degrees of change, and the secondary thermal cycle has a certain influence on impact toughness and microhardness. When the peak temperature T_{p2} is 1200 ℃, the impact toughness is still low, and its loss is 73.26 % of the base metal. Due to the existence of microstructure inheritance, the coarse grain characteristics of the CGHAZ is inherited, that is, almost no significant change happens in URCGHAZ, and the hardness is similar to CGHAZ. When the peak temperature T_{p2} is 1000 ℃, the microstructure grain is refined, and the impact toughness is significantly improved, which is similar to the base metal. Compared to the impact toughness of CGHAZ, it is increased by about 4.5 times. The microhardness is also improved, with its value increased by 19.3 % compared with that of CGHAZ. When the peak temperature T_{p2} is 800 ℃, the impact toughness loss is 67.32 % of that of the base metal. The microhardness value decreases due to the mixing of martensite and granular bainite grains. Besides, the grain size becomes inhomogeneous. When the peak temperature T_{p2} is 600 ℃, CGHAZ is subjected to high-temperature tempering treatment, which leads to the impact toughness improved nearly twice, since the internal quenching stress is eliminated during tempering, and the phenomenon of carbide precipitation and recovery of ferrite occurs. The microhardness value is lower than the hardness of the base metal and SCGHAZ shows temper softening phenomenon due to the fast heating and cooling rate.

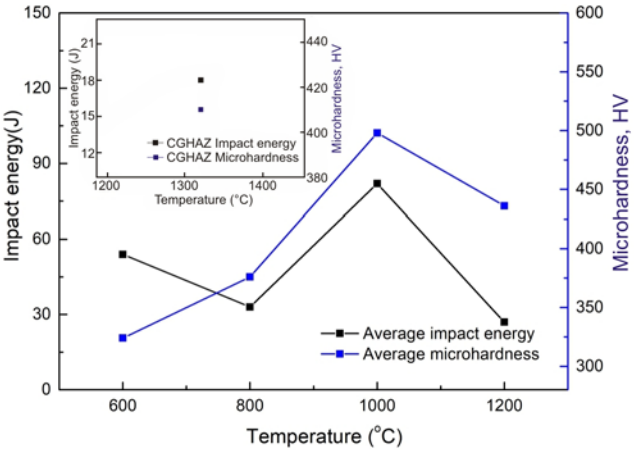

Fig. 6. Impact toughness and microhardness of RCGHAZ.

According to the above analysis, it is found that, after CGHAZ undergoes the secondary thermal cycling, URCGHAZ and IRCGHAZ become severely embrittled areas due to lower impact toughness. When the heating temperature is much higher than A_{c3}, the microstructure is transformed into coarse austenite after heating, and coarse martensite is obtained after cooling transformation. The microstructure is not improved obviously, and the impact toughness is still low.

When the peak temperature T_{p2} is 800 ℃, the microstructure of IRCGHAZ has inhomogeneous and coarse characteristic, therefore the grain size in the local area is still large. As lath martensite is heated to 800 ℃, in order to reduce the phase change resistance, the austenitic nucleus is parallel to the densely packed surface and direction of non-equilibrium microstructure. Therefore, it forms an orientational nucleation, and the austenite inherits the characteristic of coarse grain during a thermal cycle, so that the mi-

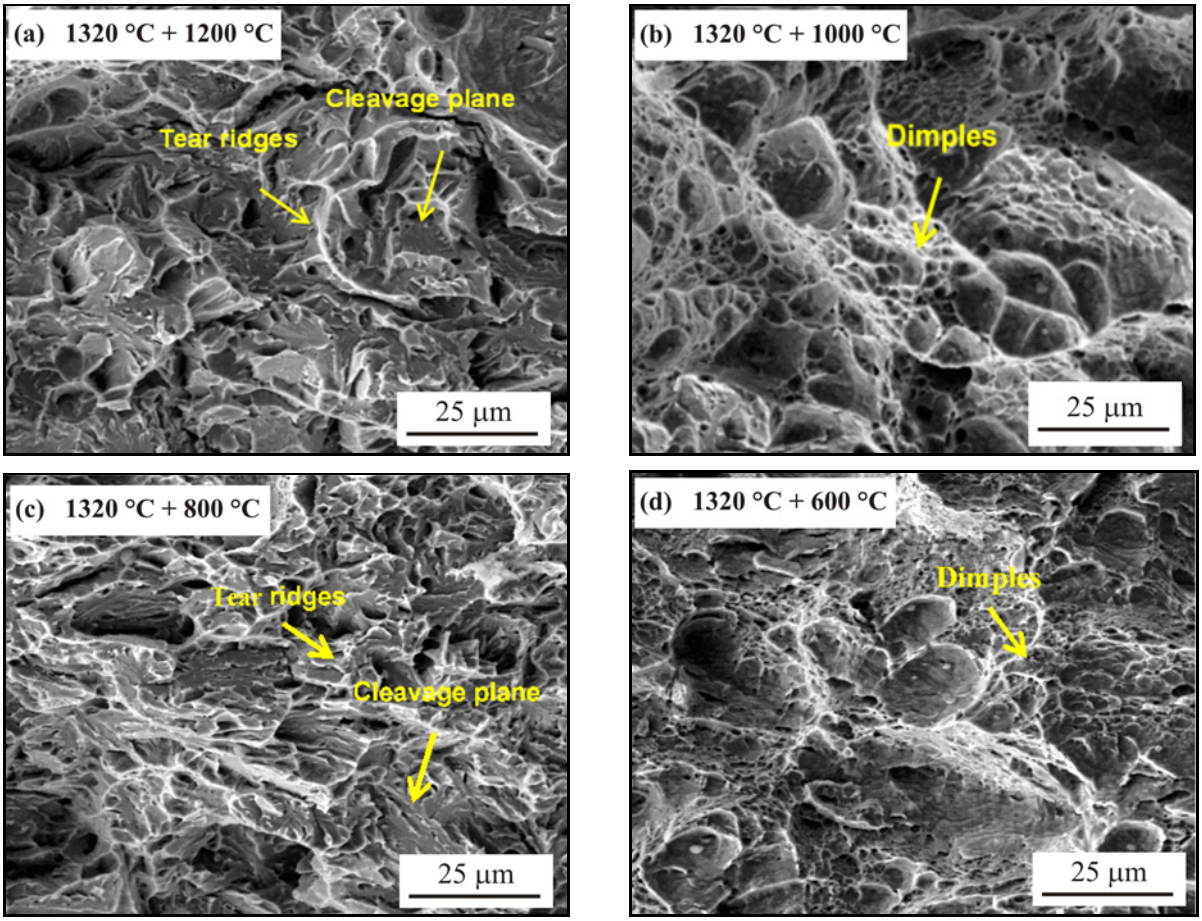

Fig. 7. Fracture morphology of RCGHAZ: 1320 + 1200 °C (a), 1320 + 1000 °C (b), 1320 + 800 °C (c), and 1320 + 600 °C (d).

crostructure has not been refined, which leads to lower toughness.

In addition, the local embrittlement of IRCGHAZ is also related to the presence of M-A constituent, which is one of the main factors causing the deterioration of impact toughness. M-A constituent has high carbon content and high hardness, and it contributes to increase brittleness and causes stress concentration. Because there is a significant difference in impact toughness between M-A constituent and base metal, stress concentration appears at the F/M-A interface, which causes caves or microcracks between the M-A constituent and base metal [21–23]. Under the action of external force, the crack is easy to generate, and brittle cracking occurs along the boundary of the M-A constituent to form a local brittle zone. The coarse grain provides thermodynamically favorable conditions for the formation of M-A constituent. The coarse austenite forms ferrite with low carbon content in the cooling process at the beginning, and some untransformed austenite with high carbon content is transformed into martensite in the following and then forms M-A constituent together with the remained austenite. The M-A constituent preferentially nucleates on the original austenite grain boundary, and it is distributed in strips between grain boundaries or between ferrite slats [24–27].

3.3. Fracture analysis

Figure 7 presents the fracture morphology of RCGHAZ at different temperatures. It can be seen that when the peak temperature T_{p2} is 1200 or 800 °C, impact samples have no obvious plastic deformation, and the surface is relatively flat with radial river pattern characteristics. The cleavage plane is large and the tearing ridge is straight, which is characterized by brittle fracture with poor impact toughness (Figs. 7a,c). When the peak temperature T_{p2} is 1000 or 600 °C, impact samples have obvious plastic deformation, and the edge of fracture has tearing edges and corners, which is characterized by ductile fracture. Through microscopic observation, the dimples are found to distribute on the fracture surface, large and small dimples coexist on the fracture surface, and some dimples are much deeper, which means better impact toughness (Figs. 7b,d).

4. Conclusions

1. When the peak temperature of secondary thermal cycle is 1200 and 1000 ℃, the microstructure of RCGHAZ is martensite; when the peak temperature is 800 ℃, the microstructure of RCGHAZ constitutes of martensite, granular bainite, and M-A constituent.

2. The impact toughness of RCGHAZ is lower than that of the base metal, and the toughness loss of URCGHAZ and IRCGHAZ is 73.26 and 67.32 % of the base metal, respectively.

3. Compared with the microhardness value of CGHAZ, the microhardness value of SCRCGHAZ increases, and the microhardness values of IRCGHAZ and SRCGHAZ decrease.

4. After the secondary thermal cycle, the impact toughness of SCRCGHAZ and SRCGHA is obviously improved, the impact fracture has obvious plastic deformation, and the microscopic morphology is characterized by dimple fracture.

Acknowledgement

The present research was financially supported by the Science and Technology Research Project of Department of Education of Liaoning Province (No. L2017LQN021).

References

[1] X. G. Zhang, The development of advanced HSLA steel in Angang in low carbon age, J. Iron Stl. Res. 18 (2011) 22–28. doi:10.1016/j.hydromet.2011.02.011

[2] W. Meng, Z. G. Li, X. X. Jiang, J. Huang, Y. X. Wu, S. J. Katayama, Microstructure and toughness of simulated heat-affected zone of laser welded joint for 960 MPa grade high strength steel, J. Mater. Eng. Perf. 23 (2014) 3640–3648. doi:10.1007/s11665-014-1137-y

[3] S. K. Sharma, S. Maheshwari, A review on welding of high strength oil and gas pipeline steels, J. Natl. Gas Sci. Eng. 38 (2017) 203–217. doi:10.1016/j.jngse.2016.12.039

[4] Y. Yang, J. S. Chen, W. J. Nie, Investigating on the microstructure and toughness of coarse grained heat affected zone in X100 multiphase pipeline steel with high Nb content, Mater. Science Eng. A 558 (2012) 692–701. doi:10.1016/j.msea.2012.08.077

[5] L. Y. Lan, C. L. Qiu, D. W. Zhao, X. H. Gao, L. X. Du, Microstructure characteristics and toughness of the simulated coarse grained heat affected zone of high strength low carbon bainitic steel, Mater. Sci. Eng. A 529 (2011) 192–200. doi:10.1016/j.msea.2011.09.017

[6] K. S. Arora, S. R. Pandu, N. Shajan, P. Pathak, M. Shome, Microstructure and impact toughness of reheated coarse grain heat affected zones of API X65 and API X80 line pipe steels, Int. J. Pres. Ves. Pip. 163 (2018) 55–62. doi:10.1016/j.ijpvp.2018.04.004

[7] S. Shanmugam, N. K. Ramisetti, R. D. K. Misra, Microstructure and high strength-toughness combination of a new 700 MPa Nb-microalloyed bridge steel, Mater. Sci. Eng. A 478 (2008) 26–37. doi:10.1016/j.msea.2007.06.003

[8] M. H. A. Musa, M. A. Maleque, M. Y. Ali, An investigation of TIG welding parameters on microhardness and microstructure of heat affected zone of HSLA steel, Mater. Sci. Eng. 290 (2018) 012041. doi: 10.1088/1757-899X/290/1/012041

[9] W. H. Sun, G. D. Wang, J. M. Zhang, D. X. Xia, H. Sun, Microstructure characterization of high-heat-input welding joint of HSLA steel plate for oil storage construction, J. Mater. Sci. Tech. 25 (2009) 857–861. doi:CNKI:SUN:CLKJ.0.2009-06-028

[10] Y. Q. Weng, C. F. Yang, C. J. Shang, The state-of-art and development trends of HSLA steels in China, J. Iron Stl. Res. Int. 18 (2011) 1–13. doi:10.1016/j.hydromet.2011.02.011

[11] M. Venkatraman, S. Majumdar, O. N. Mohanty, Modelling of strength and continuous cooling transformation behaviour of HSLA-100 plate steel, Ironmak. Steelmak. 28 (2001) 373–383. doi:10.1179/irs.2001.28.5.373

[12] M. Shome, O. P. Gupta, O. N. Mohanty, Effect of simulated thermal cycles on the microstructure of the heat-affected zone in HSLA-80 and HSLA-100 steel plates, Metall. Mater. Trans. A 35 (2004) 985–996. doi:10.1007/s11661-004-0025-8

[13] L. Y. Li, Y. Wang, H. W. Li, T. Han, C. W. Li, Embrittlement and toughness in CGHAZ of ASTM4130 steel, Sci. China Phys. Mech. 54 (2011) 1447–1454. doi:10.3354/cr00999

[14] L. G. Liang, W. S. Yang, B. H. Wu, L. X. Liu, Microstructure and mechanical performances of CGHAZ for oil tank steel during high heat input welding, Rare Metals 32 (2013) 129–133. doi:10.1007/s12598-013-0036-y

[15] Y. Chen, Microstructure and mechanical property development in the simulated heat affected zone of V treated HSLA steels, Acta Mater. 19 (2006) 57–67. doi:10.1016/s1006-7191(06)60024-0

[16] Y. W. Shi, Z. X. Han, Effect of weld thermal cycle on microstructure and fracture toughness of simulated heat-affected zone for an 800 MPa grade high strength low alloy steel, J. Mater. Process. Tech. 207 (2008) 30–39. doi:10.1016/j.jmatprotec.2007.12.049

[17] W. G. Zhao, W. Wang, S. H. Chen, J. Qu, Effect of simulated welding thermal cycle on microstructure and mechanical properties of X90 pipeline steel, Mater. Sci. Eng. A 528 (2011) 7417–7422. doi:10.1016/j.msea.2011.06.046

[18] A. L. Perlade, A. F. Gourgues, A. Pineau, Austenite to bainite phase transformation in the heat-affected zone of a high strength low alloy steel, Acta Mater. 52 (2004) 2337–2348. doi:10.1016/j.actamat.2004.01.025

[19] Y. You, C. Shang, L. Chen, S. Suramanian, Investigation on the crystallography of the transformation products of reverted austenite in inter-critically reheated coarse grained heat affected zone, Mater. Des. 43 (2013) 485–491. doi:10.1016/j.matdes.2012.07.015

[20] Z. S. Li, L. Tian, B. Jia, S. L. Li, A new method to study the effect of M–A constituent on impact toughness of IC HAZ in Q690 steel, J. Mater. Res. 30 (2015) 1973–1978. doi:10.1557/jmr.2015.154

[21] X. Li, Y. Fan, X. Ma, S. U. Subramanian, C. Shang, Influence of martensite-austenite constituents formed at different inter-critical temperatures on toughness, Mater. Des. 67 (2014) 457–463. doi:10.1016/j.matdes.2014.10.028

[22] X. D. Li, C. J. Shang, C. C. Han, Y. R. Fan, J. B. Sun, Influence of necklace-type M-A constituent on impact toughness and fracture mechanism in the heat affected zone of X100 pipeline steel, Acta Metall. Sin. 52 (2016) 1025–1035. doi:10.11900/0412.1961.2015.00610

[23] B. C. Kim, S. Lee, N. J. Kim, D. Y. Lee, Microstructure and local brittle zone phenomena in high-strength low-alloy steel welds, Metall. Trans. A 22 (1991) 139–149. doi:10.1007/bf03350956

[24] B. Cui, Y. Peng, M. D. Peng, Effects of weld thermal cycle on microstructure and properties of heat-affected zone of Q890 processed steel, Trans. China Weld. Inst. 38 (2017) 35–39. doi:10.12073/j.hjxb.20150427004

[25] S. Kumar, S. K. Nath, Effect of weld thermal cycles on microstructures and mechanical properties in simulated heat affected zone of an HY 85 steel, Trans. Indian Inst. Met. 70 (2017) 239–250. doi:10.1007/s12666-016-0880-1

[26] J. H. Chen, Y. Kikuta, T. Araki, M. Yoneda, Y. Matsuda, Micro-fracture behavior induced by M-A constituent (island martensite) in simulated welding heat affected zone of HT80 high strength low alloyed steel, Acta Metall. 32 (1984) 887–894. doi:10.1016/0001-6160(84)90234-7

[27] D. S. Liu, B. G. Cheng, Y. Y. Chen, Strengthening and toughening of a heavy plate steel for shipbuilding with the yield strength of approximately 690 MPa, Metall. Mater. Trans. 44 (2013) 440–455. doi:10.1007/s11661-012-1389-9